View metadata, citation and similar papers at core.ac.uk
brought to you by CORE
provided by University of Liverpool Repository

PHYSICAL REVIEW D **70**, 014501 (2004)

Improved Wilson QCD simulations with light quark masses

C. R. Allton,[1] A. Hart,[2] D. Hepburn,[2] A. C. Irving,[3] B. Joó,[2] C. McNeile,[3] C. Michael,[3] and S. V. Wright[3]

(UKQCD Collaboration)

[1]*Department of Physics, University of Wales Swansea, Swansea SA2 8PP, Wales*
[2]*School of Physics, University of Edinburgh, Edinburgh EH9 3JZ, Scotland*
[3]*Division of Theoretical Physics, Department of Mathematical Sciences, University of Liverpool, Liverpool L69 7ZL, England*

(Received 6 March 2004; published 9 July 2004)

We present results from simulations using 2 flavors of $\mathcal{O}(a)$-improved Wilson quarks whose masses are about 1/3 of the physical strange quark mass. We present new data on the mass of the singlet pseudoscalar meson and evidence of the onset of chiral logarithms in the pion decay constant. The previously observed suppression of the topological susceptibility at lighter quark masses is confirmed. We report on the performance of the hybrid Monte Carlo algorithm at light quark masses.

DOI: 10.1103/PhysRevD.70.014501 PACS number(s): 11.15.Ha, 12.38.Gc

I. INTRODUCTION

The first generation of QCD simulations using Wilson fermions have provided useful information on the hadron spectrum but have been restricted to relatively heavy quark masses (see for example the annual reviews by Aoki [1] and Kaneko [2]). Using an improved staggered discretization, the MILC Collaboration [3] has probed the spectrum with significantly lighter quark masses and very promising results are now being obtained [4] from simulations with light quark masses down to $m_s/8$, a physical strange quark mass m_s and lattice spacings down to 0.09 fm. There are theoretical and numerical complications associated with this action and the representation of lattice flavor symmetries and so simulations with Wilson fermions remain an important tool in studying full QCD. In due course, simulations with chiral fermions should become feasible and provide a further cross-check on the results now being obtained.

In an earlier paper [5] the UKQCD Collaboration presented lattice QCD results based on two-flavor simulations conducted at fixed lattice spacing ($a \approx 0.1$ fm) and fixed volume around $(1.6 \text{ fm})^3$. This work also contained results obtained at fixed gauge coupling ($\beta = 5.2$) also using the standard Wilson gauge action and $\mathcal{O}(a)$-improved Wilson fermions. The lightest sea quark mass achieved in these simulations was around 0.6 of the strange quark mass ($m_\pi/m_\rho \approx 0.58$). There is evidence that some hadronic observables suffer finite size effects already on these lattice volumes [6,7]. Working at lighter quark masses at fixed gauge coupling is expected to enhance further these effects and to provide an even greater challenge to the standard Monte Carlo simulation algorithms. In this paper, we report on the results of an attempt to push our analysis toward this lighter quark regime in order to (a) uncover any more obvious effects of dynamical fermions not hitherto seen with this action [5,6] and (b) determine the limits if any of the simulation algorithm in its simplest form. A previous study [8] indicated a potential instability at light quark masses when using step sizes that were too large in the molecular dynamics trajectory part of the update.

This paper should be seen as an addendum to our previous paper in which full details are given of the action, simulation methods and basic hadronic measurements. Some preliminary results from this work were presented in [9,10].

Recent related work using improved Wilson fermions includes that of the JLQCD Collaboration [6] which uses the same action and covers a similar range of quark masses to our earlier work but which also includes simulations in larger volumes [$\approx (1.8 \text{ fm})^3$]. The QCDSF Collaboration has been conducting simulations complementary to those of UKQCD, most recently using an improved algorithm [11]. Neither of these simulations sets has penetrated the lighter quark regime. In each case $m_\pi/m_\rho \geq 0.6$.

The qq+q Collaboration [12] has succeeded in simulating at one half (or less) of the strange quark mass but with rather coarse lattice spacing ($a \approx 0.28$ fm).

The rest of the paper is as follows. In Sec. II, we describe the parameters and performance of the new simulations. The lattice spacing is determined from the static potential and decorrelation effects are studied using measurements of the topological susceptibility. In Sec. III, we present the additions to our previous collection of data for the hadron spectrum and meson decay constants and use them to search for the first signs of chiral logs. Results from new measurements of disconnected loops, including the η mass, are presented in Sec. IV. We present results on the topological susceptibility in Sec. V. Conclusions are drawn in Sec. VI.

II. SIMULATIONS WITH IMPROVED WILSON FERMIONS

The simulations were conducted using the standard hybrid Monte Carlo (HMC) algorithm as described in [5] using lattice action parameters $(\beta, c_{\text{sw}}, \kappa) = (5.2, 2.0171, 0.1358)$ and a lattice volume $V = L^3T = 16^3 32$. A total of 2440 trajectories were accumulated at the rate of about 3 per hour on a machine sustaining 30 Gflops. In physical units, the lattice volume was $L^3 \approx (1.5 \text{ fm})^3$ and $m_\pi \approx 420$ MeV before chiral or continuum extrapolation. The lattice spacing was estimated from the measured hadronic scale parameter [13]:

$$r_0/a = 5.32(5). \quad (1)$$

 ©2004 The American Physical Society

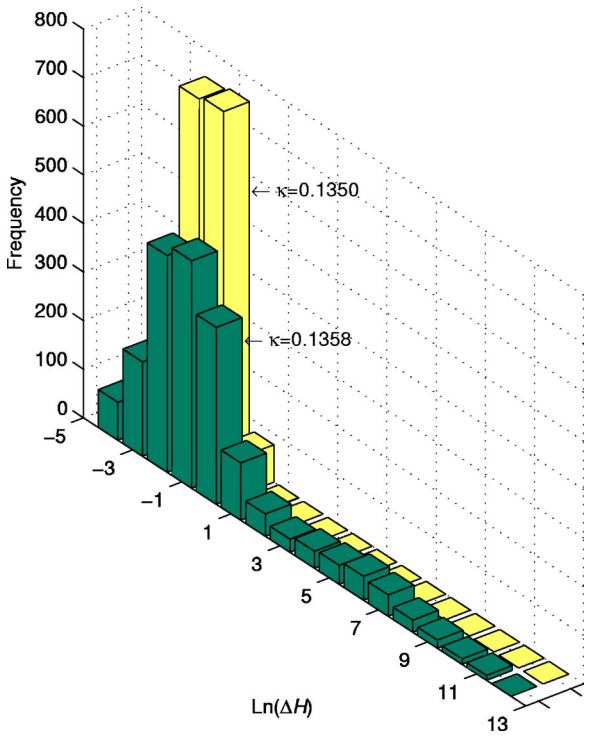

FIG. 1. Histogram of $\ln \Delta H$ (positive values of ΔH only) for this ensemble (darker bars) and for a similar sized sample from simulations at $\kappa = 0.1350$.

The integrated autocorrelation time τ of the mean plaquette was found to be 6.9(14) trajectories. This follows the previously observed trend of a *decrease* of τ with decreasing quark mass. For comparison, $\tau = 16(3)$ at $\kappa = 0.1350$ where $m_\pi / m_\rho \approx 0.7$. For the present ensemble, $m_{PS}/m_V = 0.44(2)$ (see later). Although not expected, this trend can be accommodated in simple models [5]. The mean plaquette was

$$\langle P \rangle = 0.53767(3). \tag{2}$$

These HMC runs are expected to be susceptible to instabilities (occasional large ΔH values and zero acceptance) when the fermion force term gets too large [8]. We have observed this effect directly in the present simulations where we found it necessary to use a step size of 1/400. When the step size is this, or smaller, we found that 64 bit arithmetic for field storage and matrix-vector manipulations was required so as to avoid a serious loss of acceptance due to rounding errors (see below). This was true even though we always used full 64-bit arithmetic and careful summing techniques for the global summation in our ΔH (energy difference) calculations. Figure 1 shows a histogram of $\ln \Delta H$ for all trajectories where $\Delta H > 0$. For comparison we also show the corresponding histogram for the well-behaved simulation at $(\beta, \kappa) = (5.2, 0.1350)$ described in [5]. The sample size in each case is the same.

The anomalous trajectories leading to very large values of ΔH are clearly visible in the simulation at $\kappa = 0.1358$. The simulation was an experimental one and incorporated several changes of simulation parameters (step size and solver accuracy etc.) leading to large changes in acceptance. Thus one should bear in mind the possible consequences of this on the discussion of autocorrelation times and error analysis.

In Fig. 2 we show a time history of the mean plaquette along with the average acceptance (integrated over 10 trajectories). The dramatic drop in acceptance associated with a change to 32-bit arithmetic is clearly visible. The location of the changes are indicated by the horizontal bars. The loss of acceptance was not significantly dependent on the size of the solver residual in the molecular dynamics steps (using a running rather than absolute residual). As noted above, it was primarily dependent on the arithmetic used in the matrix-vector calculations.

Despite the rather checkered history of the configurations we decided to subject them to physics analysis. This ensemble represented an expensive investment in computer time and promised to give access to relatively light quark masses (by Wilson lattice quark standards). In view of the

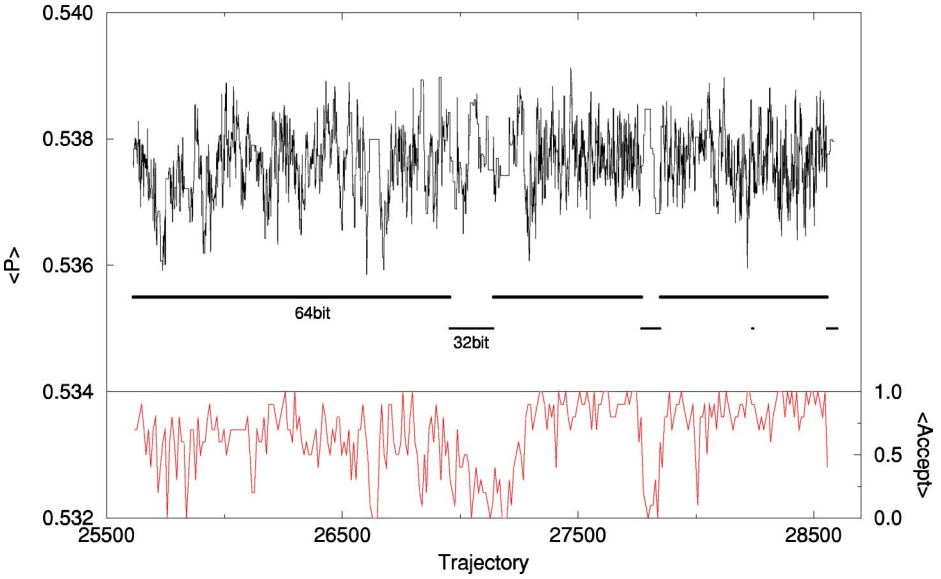

FIG. 2. The time history of the mean plaquette together with the corresponding HMC acceptance (locally averaged over 10 trajectories). The horizontal bars indicate the precision used as discussed in the text.

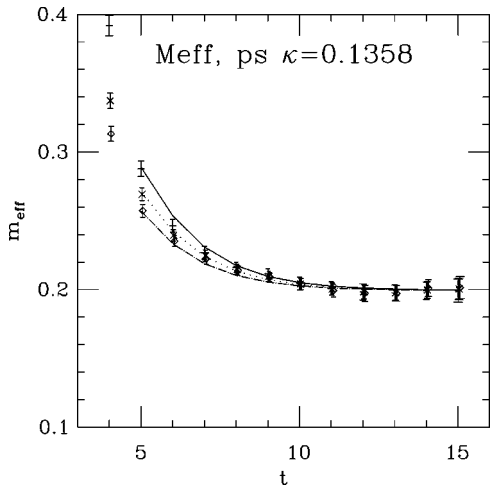

FIG. 3. Effective mass plot for the pseudoscalar channel at $\kappa = 0.1358$.

above remarks, one should bear in mind the deficiencies of the Markov process that led to their generation. We may attempt, in due course, to repeat the simulations at this lattice spacing and quark mass using improved algorithms, faster machines and larger lattices.

III. HADRON SPECTRUM AND DECAY CONSTANTS

In this section we report on the light spectroscopy from this ensemble. We use a similar analysis to our original work on the spectroscopy of nonperturbatively improved clover fermions at $\beta = 5.2$ [5]. Here we concentrate on the unitary sector of the theory—with valence quarks equal in mass to the sea quarks. We have previously reported [14] some evidence for chiral logs in a partially quenched analysis with $\kappa_{\rm sea} = 0.1355$ and $\kappa_{\rm valence} = 0.1358$. We use fuzzed and local sources and sinks combined to make a variational fit. To determine the pion decay constant, we fit with two states an order 4 variational matrix with fuzzed and local sources using the γ_5 and $\gamma_4\gamma_5$ operators to create a pion.

To increase statistics, we use quark propagators with sources on the time planes 7, 15, and 23 in addition to the $t = 0$ plane for κ values 0.1358, 0.1355, and 0.1350. In our first published work we used only the quark propagators from time plane $t = 0$. Thus we report new numbers at $\kappa = 0.1350$ and 0.1355 for π and ρ with reduced error bars.

In Fig. 3 we show the effective mass plot for the pseudoscalar channel (PS) at $\kappa = 0.1358$. The results from the fits are in Tables I and II. We investigated the stability of the fits in a number of ways. Since the spectrum fits used two states, the ground state is expected (and indeed found) to be very stable while the excited state values should be regarded as indicative, although these values are consistent with the expected lightest multi-body states at $3m_\pi$ and $2m_\pi(k = 2\pi/L)$, for the pseudoscalar and vector, respectively.

Our values of $m_\pi L \approx 4$, so we should expect some finite volume effects. Using a similar formalism and parameters (the only difference being to use $c_{\rm sw} = 2.02$ rather than 2.0171), JLQCD [6] have explored this for the hadron spectrum using $L = 12,16,20$. Here we discuss this at their lightest κ value (0.1355), where they do see evidence of a finite size effect (masses lower at larger volume) although it is not very significant statistically for the two larger volumes. We have a larger number of trajectories at $L = 16$ than JLQCD, and there are some statistically significant differences between our results [5] and theirs for that volume. However, for the pseudoscalar and vector mesons, the differences between our new determinations at $L = 16$ (given above) and theirs at $\kappa = 0.1355$ are not statistically significant. Using our newer results to make the comparison with $L = 20$ and $L = 16$, then suggests that there is a decrease of the pion mass as the volume increases by about $(4 \pm 2)\%$.

TABLE I. Masses in lattice units from this calculation.

κ	Hadron	t range	am_0	am_1
0.1358	0^{-+}	4–15	0.199(5)	0.75(11)
0.1358	1^{--}	4–12	0.450(14)	1.16(6)
0.1355	0^{-+}	4–15	0.282(4)	0.90(11)
0.1355	1^{--}	4–12	0.491(7)	1.17(3)
0.1350	0^{-+}	4–15	0.408(2)	1.19(8)
0.1350	1^{--}	4–12	0.585(4)	1.33(3)

We have also computed the pion decay constant for this data set. It has been clear from the work of the GF11 group that the unquenching effects are larger in decay constants than for masses [15], although the systematic errors on decay constants can be large due to truncation of perturbative series. The ratio f_K/f_π (for which renormalization factors should largely cancel) is underestimated in quenched lattice QCD [16].

A critical goal of lattice gauge theory calculations is to detect the presence of chiral logs in observables. The loop corrections from chiral perturbation are non-analytic in the parameters of the lowest order chiral Lagrangian, and hence provide a good check that the lattice calculation is in the regime where chiral perturbation theory is valid. A particularly appropriate way to look for these chiral logarithms is in the pseudoscalar decay constant.

We are working, because of computational constraints, at finite lattice spacing. The formalism of chiral perturbation theory can be extended to cover this case [17,18], but at the cost of additional parameters. We choose instead to make a comparison with the continuum predictions of chiral perturbation theory.

Our results for f_π are shown in Fig. 4. We have extracted the values from fits as discussed above and then applied the rotations and corrections appropriate for an order a improved

TABLE II. The raw lattice value of af_π is given by using the order a improved expression $(1 + b_A m)(af_A + c_A af_P)$ and we tabulate these two contributions.

κ	af_A	af_P
0.1358	0.0829(26)	0.1457(78)
0.1355	0.1055(14)	0.1835(44)
0.1350	0.1336(11)	0.2468(33)

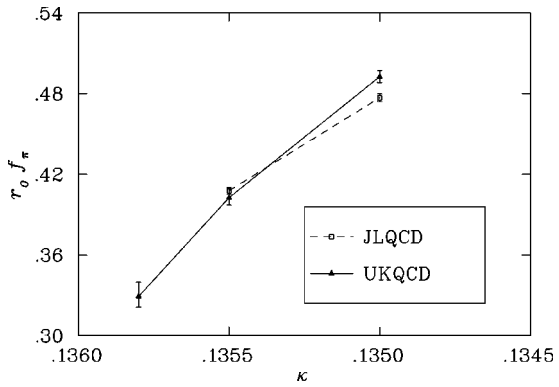

FIG. 4. The pseudoscalar decay constant in units of r_0 from UKQCD and JLQCD versus κ.

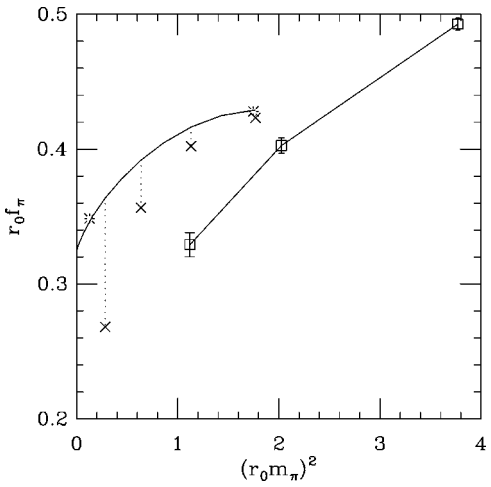

FIG. 5. The pseudoscalar decay constant in units of r_0 from UKQCD versus the squared pseudoscalar meson mass. Also shown is an expression including chiral perturbation theory terms to order m^4 which has been fitted [see Ref. [19] where we use $\mu = 0.75$ GeV and $\tilde{r}_F(\mu) = -2$] to agree with the experimental values of f_π and f_K which are shown (*). An estimate [19] of the finite size effect expected from chiral perturbation theory (to order m^2) is shown by the vertical lines.

formalism. We have used the same perturbative formulation of these corrections (and also the same prescription for Z_A) as employed by JLQCD, in order to facilitate comparisons. Moreover, since they use a different prescription for evaluating r_0, we have applied our determination of r_0 to their data. The comparison is shown in Fig. 4. The agreement at our two common κ values is adequate and we present here a new determination at a lighter κ value. The significant feature of this new result is that it shows a curvature versus m_q.

This curvature may be the first evidence in this study of the chiral logarithm at work. To explore this we compare our result with some continuum chiral models for which the chiral logarithm has a fixed coefficient (given by f_π). For $N_f = 2$ flavors of degenerate quarks, the standard chiral perturbation theory result to one loop is

$$\frac{f_\pi(m)}{f_\pi(0)} = 1 - 2\left(\frac{m}{4\pi f_\pi(0)}\right)^2 \log\left(\frac{m^2}{\Lambda^2}\right) + O(m^4). \qquad (3)$$

This expression has an unsatisfactory behavior at large m, where chiral perturbation theory should not apply anyway. Moreover, even at the K mass, the quartic terms in a chiral perturbative treatment are significant [19]. We can thus either concentrate on the curvature implied at small m or modify the expression phenomenologically. We illustrate this behavior in Fig. 5 by using an empirical determination [19] of the terms arising in chiral perturbation theory up to m^4. This shows the curvature to be expected at small pseudoscalar mass in a large volume. Unfortunately the overlap between our data and the region of validity of the chiral approach to this order is small.

As discussed above, finite volume effects should be important, since for this lightest quark mass, we have $m_\pi L = 3.2$. As has long been known, continuum chiral perturbation theory in a finite volume gives explicit predictions. This has been explored theoretically [19] using a range of different treatments of the chiral formalism, showing that we are in the region where chiral models do give rise to significant effects. Moreover the finite size effects arise from chiral loops and so are from the same source as the logarithmic corrections. Using $L = 1.5$ fm and $m_\pi = 400$ MeV, which are close to our values, a range of different levels of approximation yields [19] a relative increase of the finite-volume pion mass over the infinite volume mass of 0.6% to 2%. This can be compared to the shift of $(4 \pm 2)\%$ obtained from lattice comparisons, as discussed above. This is not a statistically significant comparison, but it does indicate that the magnitude of finite size effects to be expected theoretically is consistent with that seen on the lattice.

In the Gasser-Leutwyler chiral approach, the relative finite size effects for f_π will be four times as large as those for the pion mass, and of opposite sign. Again, this finite size effect comes from the one loop term that gives the chiral logarithm. We show the effect of this shift for the Gasser-Leutwyler approach [19–22] (corresponding to 3.4% for the above values of $L = 1.5$ fm and $m = 400$ MeV) in Fig. 5. Note that the curvature we observe is equivalent to a decrease of f_π at $\kappa = 0.1358$ of about 8%, which could thus be ascribed entirely to finite size effects only if the one loop estimate was less than 50% of the total. Since the finite size estimates come from chiral models, they will also include a chiral logarithm which will yield curvature.

We conclude that the finite volume effects will enhance the curvature at small pion masses, as indeed we find. Hence our results are in qualitative agreement with chiral perturbation theory.

We note that our data suggests an extrapolation to the chiral limit which would give a value for f_π below the experimental value of 131 MeV. Since the perturbative correction to Z_A is of order 25% at first order, we expect possible systematic errors of up to 5% from the next order, which is only estimated by using tadpole-improved methods. This error budget for Z_A is confirmed by results from quenched studies where the non-perturbative evaluation of Z_A gave a value 4% different from the tadpole-improved one loop result used here. We chose to use a value of $r_0 = 0.525$ fm to set the scale following previous work [5,23] and this value is

uncertain to 5%. There are further errors in the lattice determinations coming from having a sea quark mass which is too large, from neglect of the strange sea and from finite a effects (as well as the finite volume effects we have discussed above). This covers the apparent discrepancy of 10% seen in the figure comparing our result to the experimental values of f_π and f_K.

Although it may appear that reproducing f_π and f_K from lattice QCD has no immediate experimental impact, that is not quite true. The search for chiral logs in decay constants is currently one of the most important topics in heavy-light physics [24,25]. The error on the ratio of the f_{B_s}/f_B has recently been increased, because the chiral log term has not been observed in lattice data [26]. The ratio f_{B_s}/f_B is an important QCD quantity for the unitarity checks of the Cabibbo-Kobayashi-Maskawa matrix. It will become more important once B_s mixing is measured at run II of the CDF experiment. As has been noted by many authors [27,28], the chiral log structures of f_π and f_B are rather similar. Hence, a detection of chiral logs in f_π is an indication that the parameters of the unquenched calculation are close to where chiral logs may occur in the heavy-light decay constant.

Evidence for chiral logs in both heavy and light QCD has been claimed in unquenched calculations with improved staggered quarks [29]. Particularly because of the complexity of the chiral perturbation theory calculations for staggered fermions [30,31], we feel a cross-check on the improved staggered calculations is very valuable, even if ultimately unquenched clover fermions do not allow us to control all the systematic errors such as lattice spacing dependence.

IV. THE MASS OF THE SINGLET PSEUDOSCALAR

The large splitting between the mass of the η' and the octet of light pseudoscalars is thought to be caused by the complex vacuum of QCD and the anomaly in the axial current. There is a lot of activity in trying to reconcile the mechanism behind the mass splitting between the mass of the η' and the masses of the octet. In particular the questions raised by Witten about the consistency of the solution of the $U(1)$ via instantons with the large N_c limit [32] is topical. There are also many phenomenological puzzles in which the η' is involved. See the review by Bass [33] for a review of experiments with η and η' as decay products. A first principles calculation of the structure of the η' would be helpful.

In the real world the mass of the η' is also determined by the mixing between the singlet and octet mesons. We introduce the notation: NP is the nonsinglet pseudoscalar and SP is the singlet pseudoscalar. This mixing can be estimated from partially quenched two flavor QCD [34].

We use a similar methodology to that used in a earlier study on a coarser lattice [34]. The fermion loop was computed using complex Z_2 noise using the ''two-source'' trick we used in the calculation of the non-singlet scalar [35]. We used 100 noise samples. Using fuzzed smearing functions as a basis, we fitted to a 2×2 matrix of correlators using ''factorizing fits.'' The A_4 operator also couples to the pion so we sometimes use a basis of 4 smearing functions. To show the quality of data we plot the ratio of disconnected to connected correlators in Fig. 6. Note that unitarity requires that the SP correlator $(C-D)$ is positive so that $D/C<1$, as we do indeed find.

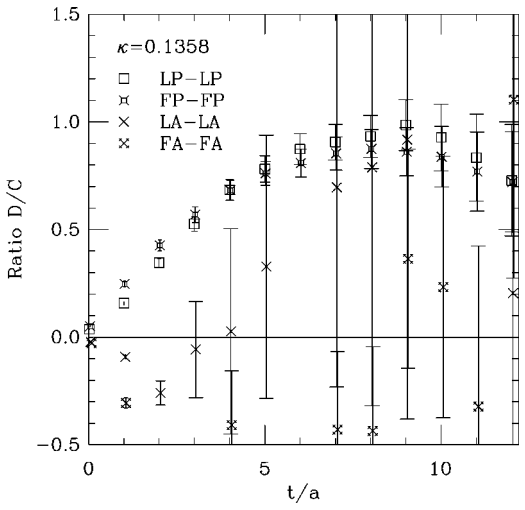

FIG. 6. The ratio of disconnected D to connected C contributions to the SP two-point correlator $(C-D)$ at $\kappa=0.1358$. The operators used for the pion are local (L) or fuzzed (F) and either γ_5 (P) or $\gamma_5\gamma_4$ (A).

The results from the fits are in Table III. As expected, the fits with a larger basis of smearing functions have smaller error bars.

For the fits to the $\kappa=0.1355$ data we could obtain a fit with three exponentials. We regard the last exponential as representing the truncation error; hence we have information on one excited state. The mass of the excited state at $\kappa=0.1355$ is 1.5(2) GeV with unknown systematic errors from the lack of continuum extrapolation and chiral extrapolation. This is encouragingly close to the mass of the $\eta(1295)$ and $\eta(1440)$ mesons. When the systematics in the lattice calculation are under control, the comparison with experiment will also require an understanding of the mixing.

For the $\kappa=0.1358$ data, we are unable to obtain convincing and consistent fits. Those shown illustrate the problem. We use a different method to show the impact of the data: namely a direct comparison between the SP correlators at the two kappa values (see Fig. 7). For the LL and FF correlators

TABLE III. Fits to the SP particle. Correlators LL, FL and FF are used in each case with (a) having PP only, (b) having PP, AP and AA, while (c) has all of PP, AP, PA and AA, where P is the pseudoscalar coupling (γ_5) and A is the time component of the axial ($\gamma_5\gamma_4$). The symbol 1 implies momentum=1. DOF indicates the degrees of freedom.

κ	Correlator	region	am_0	am_1	am_2	χ^2/DOF
0.1358	a	2–9	0.497^{+238}_{-137}	1.21^{+35}_{-12}	—	1.5/18
0.1358	b	2–9	0.623^{+72}_{-80}	1.965^{+204}_{-225}	—	34/46
0.1355	a	2–9	0.489^{+76}_{-83}	1.45^{+16}_{-16}	—	5.3/18
0.1355	c	2–9	0.432^{+37}_{-40}	0.75^{+12}_{-12}	2.10^{+25}_{-25}	48/65
0.1355	b1	2–9	0.554^{+40}_{-42}	1.09^{+40}_{-42}	1.98^{+9}_{-9}	28/41

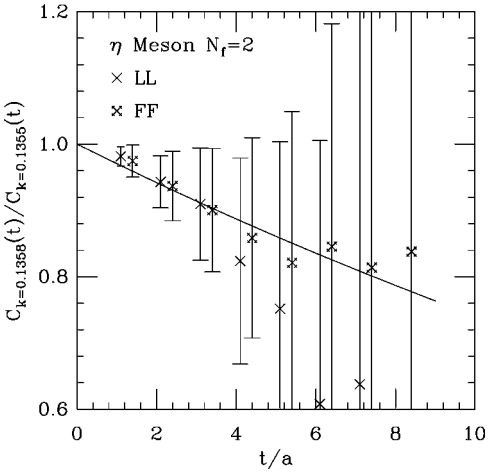

FIG. 7. The ratio of SP ($N_f=2$ η meson) two point correlations from $\kappa=0.1358$ to $\kappa=0.1355$. The curve is described in the text.

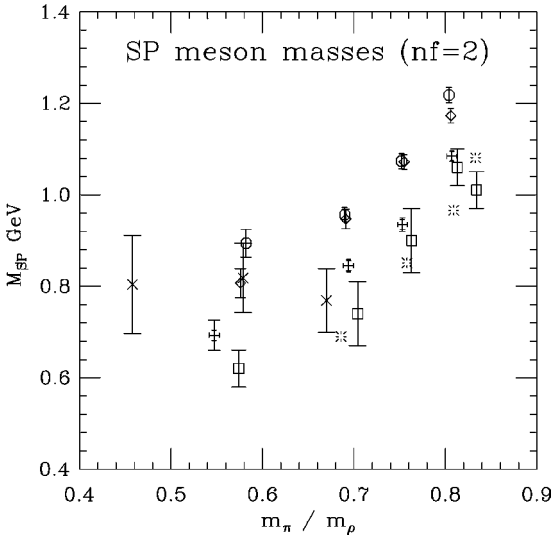

FIG. 8. World eta data from lattice studies with two degenerate sea quarks. The bursts and squares are the values from SESAM from the truncated eigenvalue analysis [41] and $Z2$ noise measurements [36] respectively. The crosses are from UKQCD ($\kappa=0.1355$ and $\kappa=0.1358$ from this work and $\kappa=0.1398$ from Ref. [34]). Results from CP-PACS [37] are shown by a diamond at $\beta=2.1$, an octagon at $\beta=1.95$ and a fancy plus at $\beta=1.8$.

(with γ_5 at source and sink) the ratios are consistent with $am_{SP}(0.1358)-am_{SP}(0.1355)=-0.03(3)$ as shown, where we have relied more on the FF data since it has a larger contribution from the ground state. This mass difference can then be used to extract an estimate of the SP mass at $\kappa=0.1358$ of $am_{SP}=0.40(5)$. Note that although the SP mass is approximately constant as the quark mass is reduced, the pion mass (in lattice units) decreases by about 0.09 and thus the difference between the SP mass and the pion mass increases. This large mass splitting is consistent with the steep rise shown in Fig. 6.

Because the signal to noise is so poor, we also explore singlet correlators with non-zero momentum. One has to be careful since, at non-zero momentum, the axial (A_4) pion operator (g_5g_4) has contamination from a_1—so factorizing fits need additional care for the A_4A_4 term. For $\kappa=0.1355$, we can fit for momentum (1,0,0) (in units of $2\pi/L$). For $\kappa=0.1358$, we find no useful additional constraint from the momentum non-zero correlators.

The mass of the SP meson in two flavor QCD is not immediately available from experiment since the well known mixing between the η and η' obscures this issue. By assuming some mixing scheme, we can obtain an estimate of the mass of the SP particle. In our previous analysis [34], the mass of the SP meson was $m_0=\sqrt{m_{ss}^2+2x_{ss}}$. Using values consistent with phenomenology and our previous lattice data ($m_{ss}=0.695$ GeV, $x_{ss}=0.13$ GeV^2), we obtained 0.861 GeV as the mass of the SP meson in $N_f=2$ QCD.

Another approach is to use the Witten-Veneziano expression. The SESAM/$T\chi L$ Collaboration [36] obtain 715 MeV for the mass of the SP in $N_f=2$ QCD.

The chiral extrapolation formulas used in the lattice QCD literature [36,37] have used either the mass or the square of the mass of the SP meson linear in the quark mass. It would be clearly better to have a more theoretical justification of the light quark mass dependence, although ''traditional'' chiral perturbation theory is not reliable at mass scales appropriate to the SP state [38,39].

In Fig. 8, the world data for the SP mass are plotted as a function of the pseudoscalar to vector mass ratio. Our point at $\kappa=0.1355$ is consistent with the data from other groups. The mass at $\kappa=0.1358$ lies above the trend from larger quark mass, but we do expect the SP mass to go to a non-zero constant as the quark mass vanishes. Indeed our semi-phenomenological estimate given above was that the SP mass in the chiral limit is 861 MeV. This value is very consistent with the flattening behavior indicated by our data point.

For their final result, CP-PACS [37] quoted the mass of the SP particle as $0.960(87)^{+0.036}_{-0.248}$ GeV. This high value arises from the continuum extrapolation. The central value for the mass was obtained by linearly extrapolated in lattice spacing with a χ^2/DOF of 4.2. A quadratic extrapolation in the lattice spacing had a χ^2/DOF of 2.8, with the resulting mass of 0.819(50) GeV. The use of a linear extrapolation with lattice spacing is consistent with the rest of the spectroscopy program of CP-PACS [40]. The large errors in the mass of the SP meson from CP-PACS represent the variation from the different continuum extrapolations.

V. TOPOLOGY

The topological charge, Q, and its associated susceptibility,

$$\chi=\frac{\langle Q^2\rangle}{L^3T}, \tag{4}$$

are expected to be especially sensitive to the presence and properties of the sea quarks in QCD. As the mass of the sea quarks is reduced (toward the chiral limit), the topological

susceptibility is suppressed below its quenched value. For sufficiently large volumes, the leading order chiral behavior is [42–44]

$$\chi(m_\pi^2) = \frac{(f_\pi m_\pi)^2}{4} + \mathcal{O}(m_\pi)^4 \tag{5}$$

for two degenerate flavors (and using a normalization where $f_\pi \simeq 93$ MeV). As $m_q \to \infty$, $\chi \to \chi^{\mathrm{qu}}$, the quenched value, which is around $(180\ \mathrm{MeV})^4$. The higher order corrections in Eq. (5) must therefore introduce a negative curvature at some intermediate quark mass [44–46].

On the lattice, the topological susceptibility becomes renormalized relative to the continuum value, χ_{cont}, both multiplicatively and additively [47]:

$$\chi = Z^2 \chi_{\mathrm{cont}} + M. \tag{6}$$

Broadly speaking, $M \geqslant 0$ arises from the presence of ''dislocations:'' short range fluctuations in the gauge field that masquerade as small instantons. $Z \leqslant 1$ reflects the breaking of scale invariance on the lattice, whereby small instantons have a topological charge less than unity. At large quark masses (or in the quenched theory) the first term in Eq. (6) dominates, suppressing χ at non-zero a. In the chiral limit, however, M dominates and is non-zero even after smoothing. The topological susceptibility then shows strong discretization effects that act to *increase* χ at finite lattice spacing.

While comparing ''matched'' ensembles at fixed lattice spacing will control discretization effects, these opposite trends imply that they will not cancel away entirely. The net effect is that any chiral suppression of the topological susceptibility at given a relative to the quenched value at an equivalent lattice spacing will be less than in the continuum limit.

We measure Q using the method of [45]: $n_c = 10$ cooling sweeps are applied using the Wilson gauge action. Ten cools strikes a good balance between adequate suppression of these ultraviolet dislocations and excessive destruction of the long range topological structure [45]. A reflection-symmetrized ''twisted plaquette'' lattice topological charge operator is used [48].

As discussed previously, good decorrelation of Q is seen in the simulation, and the histogram of the populations of the different topological sectors in Fig. 9 has the expected Gaussian form. We find $\langle Q \rangle = -0.33(29)$, consistent with zero. The susceptibility is $\chi = 0.292(45) \times 10^{-4}$, or $0.284(34) \times 10^{-4}$ if we subtract terms in $\langle Q \rangle$. We plot the latter result as the leftmost point in Fig. 10, alongside previously published UKQCD results [5,45,48–51]. We show also the equivalent quenched susceptibility as a bar whose length reflects both the statistical uncertainty in the quenched measurements and the small variation in lattice spacing across the ensembles depicted. We see very clear evidence for a strong chiral suppression of χ relative to the quenched theory, driven by the sea quarks.

For Eq. (5) to hold, we require $x_{\mathrm{LS}} \equiv (f_\pi m_\pi)^2 V \gg 1$ [44]. Using the continuum value of f_π (which is lower than the value at finite lattice spacing) we find $x_{\mathrm{LS}} = 11$. Finite volume effects appear to be less significant for χ than, for instance, the light hadron spectrum. Studies for this action indicate that $x_{\mathrm{LS}} \gtrsim 10$ is sufficient for such finite size effects to be within the statistical uncertainty in χ [52].

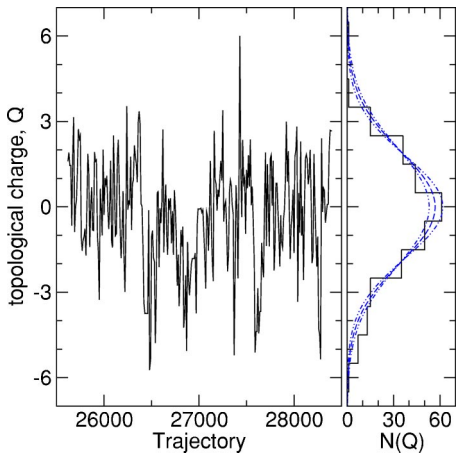

FIG. 9. A time history of the topological charge, Q, with a histogram using unit-sized bins, and the Gaussian curve derived from the central value of topological susceptibility (and one standard deviation either side as outlying curves).

As discussed above, comparison of data at finite lattice spacings with continuum predictions must be made cautiously. That being said, Fig. 10 is very encouraging and is evidence for the improved chiral properties of the $\mathcal{O}(a)$-improved action. Performing a leading order [in $(r_0 m_\pi)^2$] fit, or an interpolating fit across the chiral range [50], we see that the slope near the origin of Fig. 10 is slightly greater than that expected from the continuum value of f_π. As discretization effects are expected to increase the pseudoscalar decay constant, this is in agreement with theoretical expectations. In a forthcoming paper discretization effects will be examined in more detail [52].

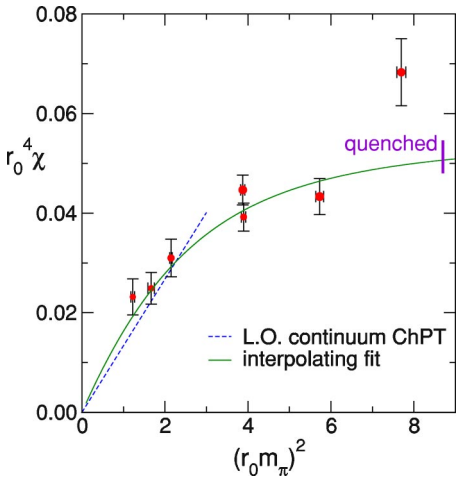

FIG. 10. The topological susceptibility as a function of the lightest pseudoscalar (''pion,'' $\kappa_{\mathrm{valence}} = \kappa_{\mathrm{sea}}$) mass for two flavors of $\mathcal{O}(a)$-improved fermions. Quenched values for this range of lattice spacing are shown as a bar on the right-hand side of the plot.

Finally, it is interesting to compare these results with those obtained for three flavors of improved staggered sea quarks [47]. For similar lattice spacings, $a \simeq 0.09$ fm, the topological susceptibility was non-zero and roughly constant below $(r_0 m_\pi)^2 \simeq 2$, when χ presumably became dominated by M. No statistically significant evidence for such a trend can yet be seen for the $\mathcal{O}(a)$-improved action, however.

VI. CONCLUSIONS

Although we are excited to have finally reached a region of parameter space where unquenched clover calculations are starting to see chiral logs and uncover interesting behavior in the mass of the singlet pseudoscalar meson, it is not yet clear how to improve on these results.

If we implemented some of the new updating algorithms [53,54] for clover fermions, in principle we could work at a larger volume with fewer of the problems reported in Sec. II. However, concerns have been raised about the interaction [55,56] of the Wilson gauge action with the clover fermion action in unquenched calculations. Once improved gauge actions have been incorporated into the non-perturbative clover improvement formalism for fermions, we could study the chiral log structure, at fixed lattice spacing [17,18]. This would allow important comparisons with the results from other unquenched lattice QCD calculations that use different fermion formalisms [4].

ACKNOWLEDGMENTS

We acknowledge the support of the U.K. Particle Physics and Astronomy Research Council under grants GR/L22744, GR/L29927, GR/L56374, PPA/G/O/1998/00621, PPA/G/O/1998/00518, PPA/G/S/1999/00532, PPA/G/O/2000/00465, and PPA/G/O/2001/00019. A.H. is supported by the U.K. Royal Society. We thank EPCC for time on Lomond. We are grateful to the ULgrid project of the University of Liverpool for computer time. The authors acknowledge support from EU grant HPRN-CT-2000-00145 Hadrons/Lattice QCD.

[1] S. Aoki, Nucl. Phys. B (Proc. Suppl.) **94**, 3 (2001).
[2] T. Kaneko, Nucl. Phys. B (Proc. Suppl.) **106**, 133 (2002).
[3] C.W. Bernard *et al.*, Phys. Rev. D **64**, 054506 (2001).
[4] HPQCD Collaboration, C.T.H. Davies *et al.*, Phys. Rev. Lett. **92**, 022001 (2004).
[5] UKQCD Collaboration, C.R. Allton *et al.*, Phys. Rev. D **65**, 054502 (2002).
[6] JLQCD Collaboration, S. Aoki *et al.*, Phys. Rev. D **68**, 054502 (2003).
[7] QCDSF Collaboration, A. Ali Khan *et al.*, Nucl. Phys. B (Proc. Suppl.) **119**, 419 (2003).
[8] UKQCD Collaboration, B. Joo *et al.*, Phys. Rev. D **62**, 114501 (2000).
[9] UKQCD Collaboration, A.C. Irving, Nucl. Phys. B (Proc. Suppl.) **119**, 341 (2003).
[10] UKQCD Collaboration, D.J. Hepburn, Nucl. Phys. B (Proc. Suppl.) **119**, 338 (2003).
[11] QCDSF Collaboration, A. Ali Khan *et al.*, Phys. Lett. B **564**, 235 (2003).
[12] qq+q Collaboration, F. Farchioni, C. Gebert, I. Montvay, E. Scholz, and L. Scorzato, Phys. Lett. B **561**, 102 (2003).
[13] R. Sommer, Nucl. Phys. **B411**, 839 (1994).
[14] UKQCD Collaboration, A.C. Irving, C. McNeile, C. Michael, K.J. Sharkey, and H. Wittig, Phys. Lett. B **518**, 243 (2001).
[15] F. Butler, H. Chen, J. Sexton, A. Vaccarino, and D. Weingarten, Nucl. Phys. **B421**, 217 (1994).
[16] ALPHA Collaboration, J. Heitger, R. Sommer, and H. Wittig, Nucl. Phys. **B588**, 377 (2000).
[17] S. Aoki, Phys. Rev. D **68**, 054508 (2003).
[18] O. Bar, G. Rupak, and N. Shoresh, hep-lat/0306021.
[19] G. Colangelo and S. Durr, Eur. Phys. J. C **33**, 543 (2004).
[20] J. Bijnens, G. Colangelo, G. Ecker, J. Gasser, and M.E. Sainio, Phys. Lett. B **374**, 210 (1996).
[21] J. Bijnens, G. Colangelo, G. Ecker, J. Gasser, and M.E. Sainio, Nucl. Phys. **B508**, 263 (1997).
[22] J. Bijnens, G. Colangelo, and P. Talavera, J. High Energy Phys. **05**, 014 (1998).
[23] UKQCD Collaboration, A. Dougall, R.D. Kenway, C.M. Maynard, and C. McNeile, Phys. Lett. B **569**, 41 (2003).
[24] N. Yamada, Nucl. Phys. B (Proc. Suppl.) **119**, 93 (2003).
[25] A.S. Kronfeld, Nucl. Phys. B (Proc. Suppl.) **129-130**, 46 (2004).
[26] A.S. Kronfeld and S.M. Ryan, Phys. Lett. B **543**, 59 (2002).
[27] MILC Collaboration, C. Bernard *et al.*, Phys. Rev. D **66**, 094501 (2002).
[28] D. Becirevic, S. Fajfer, S. Prelovsek, and J. Zupan, Phys. Lett. B **563**, 150 (2003).
[29] M. Wingate, C.T.H. Davies, A. Gray, G.P. Lepage, and J. Shigemitsu, Phys. Rev. Lett. **92**, 162001 (2004).
[30] C. Aubin and C. Bernard, Phys. Rev. D **68**, 034014 (2003).
[31] C. Aubin and C. Bernard, Phys. Rev. D **68**, 074011 (2003).
[32] E. Witten, Nucl. Phys. **B149**, 285 (1979).
[33] S.D. Bass, Phys. Scr., T **99**, 96 (2002).
[34] UKQCD Collaboration, C. McNeile and C. Michael, Phys. Lett. B **491**, 123 (2000).
[35] UKQCD Collaboration, C. McNeile and C. Michael, Phys. Rev. D **63**, 114503 (2001).
[36] TχL Collaboration, T. Struckmann *et al.*, Phys. Rev. D **63**, 074503 (2001).
[37] CP-PACS Collaboration, V.I. Lesk *et al.*, Phys. Rev. D **67**, 074503 (2003).
[38] R. Kaiser and H. Leutwyler, Eur. Phys. J. C **17**, 623 (2000).
[39] B. Borasoy and S. Wetzel, Phys. Rev. D **63**, 074019 (2001).
[40] CP-PACS Collaboration, A. Ali Khan *et al.*, Phys. Rev. D **65**, 054505 (2002).
[41] H. Neff, T. Lippert, J.W. Negele, and K. Schilling, Nucl. Phys. B (Proc. Suppl.) **119**, 251 (2003).
[42] R.J. Crewther, Phys. Lett. **70B**, 349 (1977).
[43] P.D. Vecchia and G. Veneziano, Nucl. Phys. **B171**, 253 (1980).
[44] H. Leutwyler and A. Smilga, Phys. Rev. D **46**, 5607 (1992).

[45] UKQCD Collaboration, A. Hart and M. Teper, hep-ph/0004180.
[46] S. Dürr, Nucl. Phys. **B611**, 281 (2001).
[47] MILC Collaboration, C. Bernard *et al.*, Phys. Rev. D **68**, 114501 (2003).
[48] UKQCD Collaboration, A. Hart and M. Teper, Nucl. Phys. B (Proc. Suppl.) **83-84**, 476 (2000).
[49] UKQCD Collaboration, A. Hart, Nucl. Phys. B (Proc. Suppl.) **106**, 575 (2002).
[50] UKQCD Collaboration, A. Hart and M. Teper, Phys. Lett. B **523**, 280 (2001).
[51] UKQCD Collaboration, A. Hart and M. Teper, hep-lat/0009008.
[52] UKQCD-QCDSF Collaboration, A. Hart, Phys. Rev. D **69**, 074510 (2004).
[53] M. Hasenbusch and K. Jansen, Nucl. Phys. **B659**, 299 (2003).
[54] M. Hasenbusch, Nucl. Phys. B (Proc. Suppl.) **129-130**, 27 (2004).
[55] K. Jansen, Nucl. Phys. B (Proc. Suppl.) **129-130**, 3 (2004).
[56] ALPHA Collaboration, R. Sommer *et al.*, Nucl. Phys. B (Proc. Suppl.) **129-130**, 405 (2004).